



SCHEDULED GAINS CONTROL APPLIED TO A DC-DC CONVERTER FOR LIGHT INTENSITY DIMMING AN LED LAMP

CONTROL POR GANANCIAS PROGRAMADAS APLICADO A UN CONVERTIDOR DC-DC PARA LA REGULACIÓN DE LA INTENSIDAD LUMINOSA DE UNA LÁMPARA LED

Gregorio Saúl Olivar-Castellanos^{1,*} , Luis Gerardo Vela-Valdés¹ ,
 Jesús Aguayo-Alquicira¹ 

Received: 12-11-2022, Received after review: 01-12-2022, Accepted: 09-12-2022, Published: 01-01-2023

Abstract

Nowadays there are several applications of LED lighting, but some of them require to precisely regulate lighting in a wide range of operation, mainly in tracking tasks. In these cases, it is necessary to consider the nonlinearity of the LED for the design of control schemes; moreover, an efficient power source is needed to supply the voltage and current variations required by the lamp. This paper presents the design of a DC-DC converter capable of implementing these variations, as well as the design, simulation and comparison of classical PI, fuzzy PI and gain-scheduling control schemes for these applications. In order to validate the described control schemes and to comply with the recommendations of the World Health Organization, the control of the illuminance produced by an eye protection lamp is taken as a case study, where the controller varies the duty cycle of the converter to adjust the voltage of the lamp, and consequently regulate the luminous intensity. Comparing the control schemes, the gain-scheduling control has a better performance for the case study described above, presenting a steady state error of 0% and lower overshoot.

Keywords: control, converter, dimming, Gain-scheduling, LED, nonlinear

Resumen

En la actualidad existen diversas aplicaciones de la iluminación LED, sin embargo, algunas de estas requieren regular la iluminación con precisión y en un amplio rango de operación, principalmente en tareas de seguimiento. Es en estos casos en donde es necesario considerar la no linealidad del LED para el diseño de esquemas de control, además, se necesita de una fuente de alimentación eficiente ante los cambios de tensión y corriente requeridos por la lámpara. En este trabajo se presenta el diseño de un convertidor DC-DC capaz de realizar y soportar estas variaciones, así como el diseño, simulación y comparación de esquemas de control PI clásico, PI difuso y ganancias programadas para estas aplicaciones. Con el fin de validar los esquemas de control descritos, y con el propósito de cumplir las recomendaciones de la Organización Mundial de la Salud, se toma el control de la iluminancia producida por una lámpara de protección ocular como caso de estudio, en donde el controlador varía el ciclo de trabajo del convertidor, ajustando de esta manera la tensión de la lámpara, y en consecuencia regulando la intensidad luminosa. Comparando los esquemas de control, el desempeño del sistema con el control por ganancias programadas tiene mejores características para el caso de estudio descrito con anterioridad, presentándose un error en estado estable de 0 % y menor sobretiro en comparación con los otros esquemas de control desarrollados.

Palabras clave: control, convertidor, ganancias programadas, LED, no lineal, regulación

^{1,*}Centro Nacional de Investigación y Desarrollo Tecnológico, Tecnológico Nacional de México, Cuernavaca, México.
 Corresponding author ✉: m21ce085@cenidet.tecnm.mx.

Suggested citation: Olivar-Castellanos, G. S.; Vela-Valdés, L. G. and Aguayo-Alquicira, J. "Scheduled gains control applied to a DC-DC converter for light intensity dimming an LED lamp". *Ingenius, Revista de Ciencia y Tecnología*. N.º 29, (january-june). pp. 66-78. 2023. DOI: <https://doi.org/10.17163/ings.n29.2023.06>.

1. Introduction

Over time, lightning has experienced various technological advances, such as the incorporation of the LED (light emitting diode) in different applications. This is mainly because LEDs have low consumption, high reliability and a larger useful life compared to other technologies, which make them a sustainable, practical and functional alternative to save energy [1].

In this technology, some applications are so simple that an On-Off control of the LED lamp is enough, but many others often require to regulate light intensity between 0% and 100% with a fine resolution [2].

There are different architectures for LED controllers, whose objective is to address the requirements and limitations posed by different lightning applications, such as indoor/outdoor lightning, greenhouse lamps, traffic signals, etc. LED controllers are often developed and adapted from basic topologies of AC-DC and/or DC-DC converters, to integrate functionalities such as precise power control or regulation of light intensity [3].

Regardless of their complexity, all power conversion systems have at least one DC-DC converter stage. The topologies of DC-DC converters most commonly used in the development of LED drivers include buck, boost, flyback, sepic and/or half-bridge converters [3].

However, there are applications in which it is essential to incorporate control schemes with the aim of improving the precision and response of the system. For this purpose, classical control schemes have been commonly used in [4–7] for regulation applications, i.e., where there is a single operating point of the LED, since they are enough to guarantee the desired dynamics around such point.

On the other hand, there are more complex applications that require stability along the entire operating range of the LED, giving rise to tracking control. Since the LED is a nonlinear device, it is required a nonlinear control strategy to have it work with precision in its entire operating range.

To address this issue, some authors have incorporated schemes based on neural networks [8], fuzzy logic [9–11], or even a combination of control schemes such as the fuzzy PID [12]. Nevertheless, most of these works focus on guaranteeing a low steady-state error, and for these cases it is enough to implement a unique nonlinear control, such as the work presented in [2]. However, there are applications where it is required to watch the maximum overshoot, besides guaranteeing a low error percentage. For this reason, another alternative has been presented in the literature to address the LED nonlinearities, such as the gain-scheduling technique together with a Flyback converter proposed in [13] for light intensity control in a LED arrangement; however, there is no specific application, and the controller is tuned empirically.

The gain-scheduling technique uses linear tools that approximate the nonlinear dynamics of the system, enabling to adjust a controller for every different operating point in advance, and subsequently update the parameters from such designs and according to the operating point of the process [14, 15].

The objective of this work is to design a supply source that regulates the light intensity of a LED lamp in a wide operating range, with low steady-state error and taking care not to damage the lamp with large overshoots. The eye protection lamps are used as a case study.

The rest of the paper is organized as follows. Section 2 presents the methodology for developing the system, which comprises from lamp characterization to tuning the control schemes. Section 3 analyzes the results obtained, and finally section 4 addresses conclusions and future works.

1.1. Case study: Eye protection lamp

According to the World Health Organization (WHO), at least 2200 million people have vision impairment or blindness, and more than 1000 million could have prevented it [16]. Some studies demonstrate that for 2050, 50% of the world population will suffer myopia, and human vision will face an increasingly severe test [17].

One of the main causes of visual impairment is myopia, which may be prevented having the appropriate lighting levels. For this reason, the WHO recommends to maintain an illuminance level of 500 lx in the study and working areas, preferably with white light sources, in order to prevent this condition [18].

This is not a simple task, since external light sources, such as natural lighting, or even other sources of artificial lightning, disturb lighting in the desired area, causing that the recommended levels are not reached.

Based on this, it is necessary a system capable of regulating the light intensity provided by an eye protection lamp, such that it complements the external lighting, maintaining the illuminance level at the 500 lx recommended by the WHO.

Taking this into account, a DC-DC converter is designed with control schemes such as classical PI, fuzzy PI and gain-scheduling, with the purpose of selecting the control scheme suitable for this case study, and thus demonstrate that a linear control scheme is not appropriate for tracking tasks in LED lighting.

2. Materials and methods

A LED is a device whose light intensity depends on the current that circulates through it [13]. Nevertheless, this current depends on the voltage across its terminals. Therefore, for varying the light intensity of a LED it is practical to vary the voltage. For this purpose, it is

necessary a supply source capable of performing and withstanding these variations.

Because of this, it is proposed to implement a DC-DC converter that fulfills these requirements. In addition, a control scheme should be incorporated to guarantee the levels recommended by the WHO. This is represented by the block diagram shown in Figure 1.

The required illuminance level is assured if it is guaranteed that the lamp voltage is the desired one. Therefore, in order to simplify the system, the different controllers are tuned considering the voltage value as a reference.

The entire process is described in subsequent sections, using Simulink/Matlab to simulate the system under the action of the controllers.

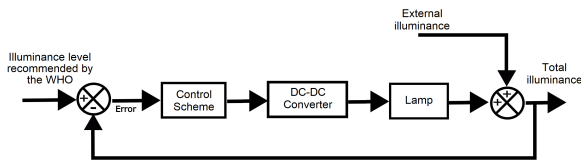


Figure 1. Block diagram of the system proposed

2.1. Lamp characterization

In order to have the eye protection lamp supplementing natural light, it is necessary to design a supply source with a controller that enables to regulate the illuminance depending on the varying conditions of natural light.

The first step is to characterize the lamp. The schematic diagram shown in Figure 2 is used for this purpose. It is known that the lamp requires an input voltage of 12 VDC; hence, such voltage is applied and then progressively reduced, measuring the changes in voltage, current and illuminance.

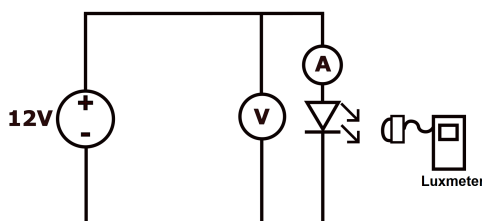


Figure 2. Circuit for characterizing the lamp

Figure 3 shows the V-I (voltage-current) curve and Figure 4 shows the V-E (voltage-illuminance) curve, both obtained plotting the measured data.

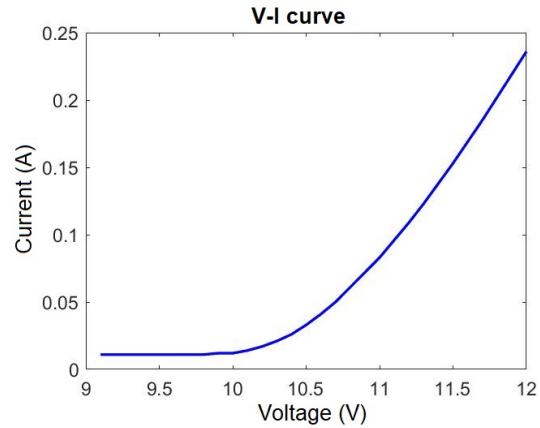


Figure 3. V-I curve of the eye protection lamp

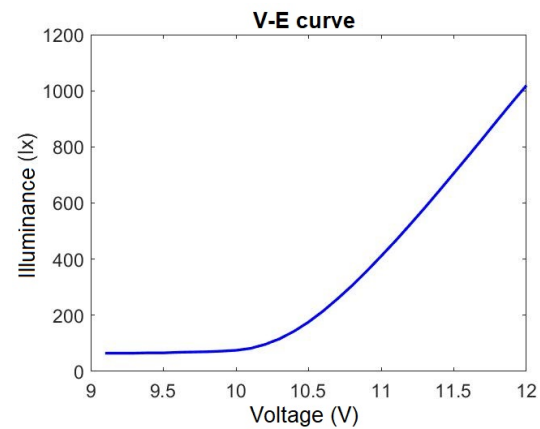


Figure 4. V-E curve of the eye protection lamp

2.2. Design of the DC-DC converter

The Buck converter is used in applications where the load requires voltages lower than the input voltage of the converter. Its implementation is simple due to the few components; in addition, its control is simple because the relationship between the output and input voltages is proportional to the duty cycle of the control signal [13].

For this reason, the Buck converter is chosen as the supply source for the lamp. The specifications shown in Table 1, which are proposed from the characterization of the lamp, are defined for the design of the converter. Figure 5 shows the topology of this converter.

Table 1. Design specifications of the converter

Parameter	Symbol	Value
Input voltage	V_{in}	24 V
Minimum output voltage	$V_{omín}$	9 V
Maximum output voltage	$V_{omáx}$	12 V
Maximum output power	$P_{omáx}$	3.5 W
Switching frequency	f_s	66.67 KHz
Current ripple in the inductor	Δ_{iL}	0.3 % $I_{omáx}$
Voltage ripple in the capacitor	Δ_{vc}	0.1 % $V_{omín}$

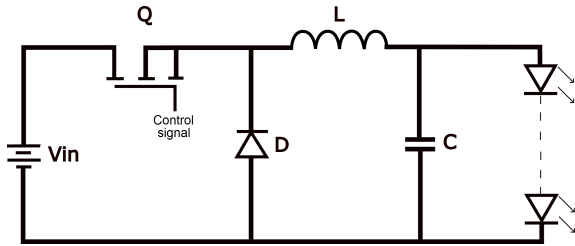


Figure 5. Topology of the Buck converter

From the analysis and the equations showed by Gamboa [19], it is made the calculation and selection of the components. Their values are shown in Table 2.

Table 2. Calculation of the components and variables of the converter

Parameter	Symbol	Value
Minimum duty cycle	D_{\min}	0.375
Maximum duty cycle	D_{\max}	0.5
Inductor	L	102.85 mH
Capacitor	C	182.29 nF
Average current through the switch	I_Q	0.146 A
Voltage across the switch	V_{DS}	24 V
Average current through the diode	I_D	0.243 A
Voltage across the diode	V_D	24 V

2.3. Transfer functions

To obtain the transfer functions (TF) it should be considered that the converter load is variable, because the LED works at different operating points according to the requirements. Therefore, it is not possible to obtain a unique linear TF that represents the entire dynamics of the system.

Based on the above and to facilitate the design of the controllers, the V-E curve is divided into five ranges approximately linear, as shown in Figure 6. After the curve is divided, it is possible to obtain five TFs that approximate the dynamics in each of those ranges.

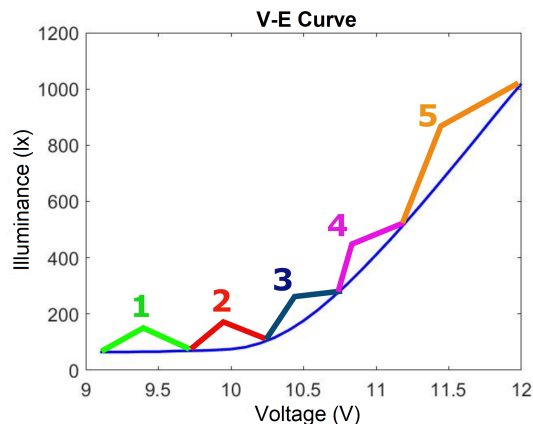


Figure 6. V-E curve divided into five ranges

Afterwards, since the operating points are defined, it is possible to obtain the TF from the control-output characteristic function of a Buck converter, shown in Equation (1).

$$G_{vd} = \frac{y(s)}{\hat{d}(s)} = \frac{V_{in} \left(\frac{1}{LC} \right)}{s^2 + \frac{1}{RC}s + \frac{1}{LC}} \quad (1)$$

Since the controller performs in the entire operating range of the lamp, the value of R in Equation (1) is variable. Therefore, an average R is calculated in each of the ranges defined, thus obtaining a different TF for each operating range. The parameters for these TFs are shown in Table 3, whereas the transfer functions are shown in Equations (2) - (6).

$$\frac{24(53337524.95)}{s^2 + 6385.48s + 53337524.95} \quad (2)$$

$$\frac{24(53337524.95)}{s^2 + 6925.77s + 53337524.95} \quad (3)$$

$$\frac{24(53337524.95)}{s^2 + 14428.63s + 53337524.95} \quad (4)$$

$$\frac{24(53337524.95)}{s^2 + 38978s + 53337524.95} \quad (5)$$

$$\frac{24(53337524.95)}{s^2 + 80507.26s + 53337524.95} \quad (6)$$

Table 3. Parameters of the transfer functions

Range	V_{in}	L	C	R	T. F.
9.2 V	24 V	102.85 mH	182.29 nF	859.10 Ω	(2)
9.7 V					
9.7 V				792.08 Ω	(3)
10.2 V					
10.2 V				380.2 Ω	(4)
10.7 V					
10.7 V	140.74 Ω	(5)			
11.3 V					
11.3 V	68.14 Ω	(6)			
12 V					

It is important to remark that having a different transfer function for each operating range implies that different dynamics are achieved in each of them. This is due to the fact that there is a different damping ratio (ζ) in each range, despite the natural frequency is the same (ω_n). This is detailed in Table 4.

Table 4. Damping ratio and natural frequency in the operating ranges

Range	T. F.	ζ	ω_n
9.2 V–9.7 V	(2)	0.437	7304.32 rad/s
9.7 V–10.2 V	(3)	0.474	7304.32 rad/s
10.2 V–10.7 V	(4)	0.988	7304.32 rad/s
10.7 V–11.3 V	(5)	2.66	7304.32 rad/s
11.3 V–12 V	(6)	5.51	7304.32 rad/s

2.4. Tuning of a PI controller

Since the PI control scheme is one of the most widely used in applications with DC-DC converters, such control scheme is tuned to validate and compare its performance in the regulation of the illuminance of an eye protection lamp.

The controller is tuned for the intermediate operating range, corresponding to the TF of Equation (4).

The pole assignment methodology is used for the tuning, considering that the characteristic equation of a second order TF may be simplified as shown in Equation (7).

$$G(s) = \frac{k}{s^2 + as + b} \quad (7)$$

In addition, it is known that the TF of a PI controller is of the form shown in Equation (8).

$$C(s) = \frac{K_c s + K_i}{s} \quad (8)$$

Then, closing the loop of the plant with the controller results in the TF shown in Equation (9).

$$H(s) = \frac{k(K_c s + K_i)}{s^3 + as^2 + (b + kK_c)s + kK_i} \quad (9)$$

Therefore, a pole assignment should be implemented based on a characteristic equation of the form shown in Equation (10), corresponding to a third order system with two complex conjugate poles and a real pole, where β represents a factor of proportionality that relates the distance of the real pole with respect to the complex conjugate poles.

$$P_d = (s + \beta\zeta\omega_n)(s^2 + 2\zeta\omega_n s + \omega_n^2) \quad (10)$$

Then, setting (10) equal to the denominator of the closed-loop TF of Equation (9) and solving for the unknowns, results in three equations useful to calculate the gains of the PI controller. is calculated using Equation (11), whereas Equations (12) and (13) are used to calculate the proportional gain (K_c) and the integral gain (K_i), respectively.

$$\beta = \frac{\alpha}{\zeta\omega_n} - 2 \quad (11)$$

$$K_c = \left(\frac{2\beta\zeta^2 + 1}{k} \right) \omega_n^2 - b \quad (12)$$

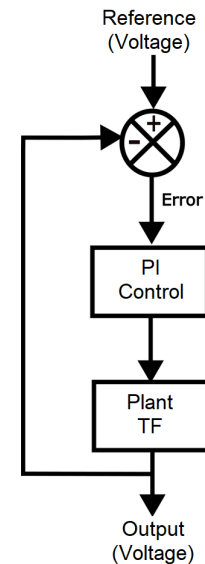
$$K_i = \frac{\beta\zeta\omega_n^3}{k} \quad (13)$$

In this manner, the gains of the PI controller may be calculated from the desired damping ratio (ζ) and natural frequency (ω_n). It is important to mention that it is possible to calculate ζ and ω_n from Equations (14) and (15), defining a maximum overshoot (M_p) and a settling time (t_{ss}). In this case, it is proposed an M_p not larger than 5 % and to search for a t_{ss} of 1 ms.

$$\zeta = \frac{\ln\left(\frac{\%M_p}{100}\right)^2}{\sqrt{\pi^2 + \ln\left(\frac{\%M}{100}\right)^2}} \quad (14)$$

$$\omega_n = \frac{4}{\zeta t_{ss}} \quad (15)$$

Therefore, it is obtained that $\beta = 1.608$, $K_c = 0.247$ and $K_i = 168.7537$. This is implemented as shown in Figure 7.

**Figure 7.** Block diagram of the implementation of the PI control

2.5. Tuning of a fuzzy PI controller

It is common that fuzzy logic control has a level of uncertainty, since it is better expressed as a control through words that interpret common sense, instead of numbers, or sentences instead of equations [20]. However, the process variables are not measured in common sense, but in numbers.

To overcome this issue, it is convenient to incorporate the gains of a PI controller to numerically correct the weaknesses of the fuzzy interpretation. The block

diagram that represents this control scheme is shown in Figure 8.

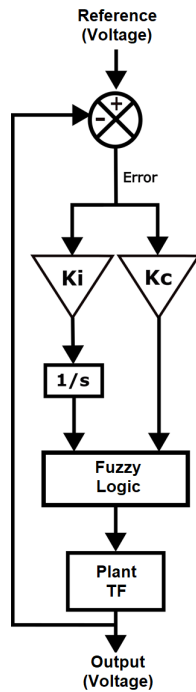


Figure 8. Block diagram of the implementation of the fuzzy PI control

The design of the fuzzy controller requires to clearly know the input and output variables. In this case, the input variables are the error and the integral of the error, and the output is the duty cycle, since this is the variable required by the plant.

Since the error is obtained through the comparison of the output of the converter, which corresponds to a maximum voltage of 12 V, it is defined a universe of discourse between $\{-12, 12\}$ for both inputs. It is important to mention that the universe defined contains negative numbers, because it is possible to obtain a positive or a negative difference between the output and the reference.

The linguistic variables defined for the error signal are:

- NE: Negative Error
- ZE: Zero Error
- PE: Positive Error

On the other hand, the linguistic variables defined for the integral of the error are:

- NIE: Negative Integral of the Error
- ZIE: Zero Integral of the Error
- PIE: Positive Integral of the Error

Once the different linguistic variables for the inputs have been established, as well as the associated universes of discourse, the corresponding fuzzy sets are defined, as shown in Figure 9 and Figure 10, respectively.

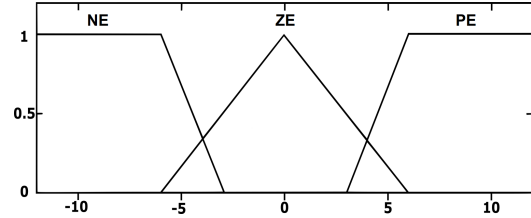


Figure 9. Fuzzy sets for the error

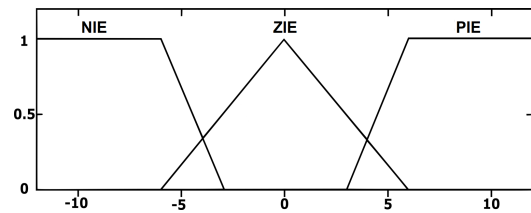


Figure 10. Fuzzy sets for the integral of the error

On the other hand, the output of the fuzzy block is the duty cycle, whose universe of discourse is defined between $\{0, 1\}$ because this is its interval of operation.

The linguistic variables defined for the duty cycle are:

- S: Small
- I: Ideal
- L: Large

The fuzzy sets of the duty cycle are shown in Figure 11.

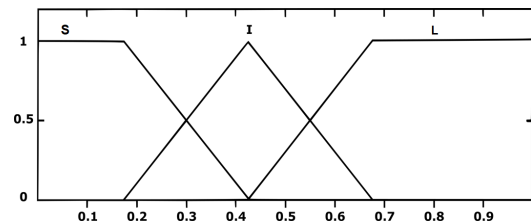


Figure 11. Fuzzy sets for the duty cycle

Once the different fuzzy sets have been defined, the control rules are assigned. For each output it is assigned an appropriate linguistic variable, based on the possible combinations of the inputs. The set of rules is shown in Table 5.

Table 5. Fuzzy rules for the output variable of the controller

		Integral of the error		
		NIE	ZIE	PIE
Error	NE	D: S	D: S	D: S
	ZE	D: I	D: I	D: I
	PE	D: L	D: L	D: L

In order to verify the performance of the fuzzy PI controller, the fuzzy sets and rules defined are uploaded in the fuzzyLogicDesigner tool.

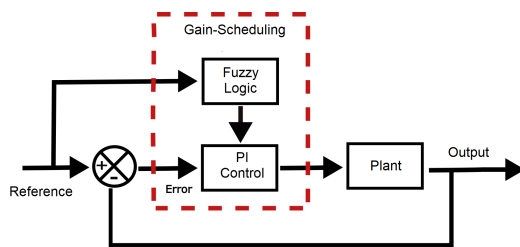
2.6. Gain-scheduling control

Gain-scheduling control consists of designing a controller for every different operating point in advance, and further selecting the controller to be implemented from such designs according to the operating point of the process [14, 15].

One of the most widely used methods for selecting the gains is fuzzy logic, which gives rise to a control strategy known as fuzzy gain scheduling [13].

In this strategy fuzzy logic is responsible for varying the gains in real-time, with the added benefit of enabling a smooth transition between the controllers determining intermediate values of the gains, and thus reducing drastic changes that may affect the controller and the plant.

Based on the above, the block diagram of Figure 12 shows the system to be implemented. The gain-scheduling control designed is constituted by a fuzzy logic block, which is responsible of choosing the gains of the PI controller depending on the operating point.

**Figure 12.** Block diagram of a gain-scheduling control

Since the operating range of the LED lamp has been divided into five intervals, there are 5 different TFs for a which a different PI controller should be designed.

Considering that each operating range has different dynamics, distinct design specifications are proposed for each of those ranges.

An important point to be taken into account is that the overshoot should not be very large in the operating range from 11.3 V to 12 V, because the LED lamp could be damaged. Based on this, Table 6 shows the design specification for each controller.

Table 6. Design specifications for the PI controllers

Range	T. F.	% M_p	t_{ss}
9.2 V-9.7 V	(2)	10%	1.5 ms
9.7 V-10.2 V	(3)	8%	1.5 ms
10.2 V-10.7 V	(4)	5%	1.5 ms
10.7 V-11.3 V	(5)	2%	5 ms
11.3 V-12 V	(6)	1%	8 ms

The pole assignment methodology described in section 2.4 is used for tuning the controllers, which gives the gains shown in Table 7.

Table 7. Gains of the PI controllers

Range	K_c	K_i
9.2 V – 9.7 V	0.0203	16.725
9.7 V – 10.2 V	0.0208	225.323
10.2 V – 10.7 V	0.0079	1.060.908
10.7 V – 11.3 V	0.0059	307.392
11.3 V – 12 V	0.0207	227.538

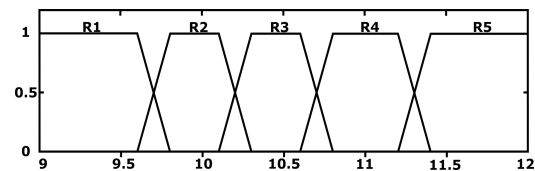
On the other hand, a fuzzy logic control is designed for selecting the gains of the PI controller.

For this case, it is convenient to have the reference signal as input variable, since it defines the working operating range. Similarly, the K_c and K_i gains are defined as output variables, since these variables vary depending on the operating range.

Taking into account the operating range, the universe of discourse of the input variable is defined as {9, 12}. On the other hand, the linguistic variables for the operating ranges are defined as:

- R1: {9.2 – 9.7}
- R2: {9.7 – 10.2}
- R3: {10.2 – 10.7}
- R4: {10.7 – 11.3}
- R5: {11.3 – 12}

Once the linguistic variables of the input have been established, the fuzzy sets shown in Figure 13 are defined.

**Figure 13.** Fuzzy sets of the operating ranges

Regarding the fuzzy sets of the output, the universe of discourse for K_c is {0.004, 0.022} and for K_i is {10, 110}.

Meanwhile, it is observed for linguistic variables that there are two ranges where the gains are very similar; consequently, these two were averaged and

defined as a single one, and thus the linguistic variables for K_c are defined as:

- Very small - MP: 0.0059
- Small - S: 0.0079
- Medium - M: 0.0203
- Large - L: 0.02075

On the other hand, the linguistic variables for K_i are defined as:

- Small – S: 16.725
- Medium – M: 22.6430
- Large – L: 30.7392
- Very Large – VL: 106.0908

Then, the fuzzy sets for the K_c gain are defined as shown in Figure 14, whereas the fuzzy sets for the K_i gain is shown in Figure 15.

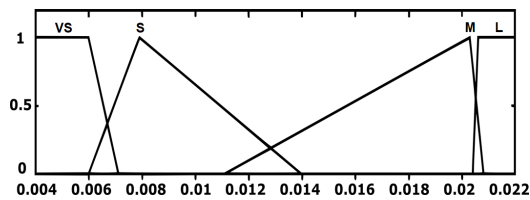


Figure 14. Fuzzy sets for the proportional gain K_c .

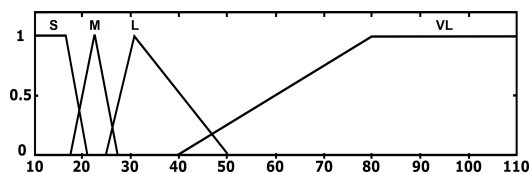


Figure 15. Fuzzy sets for the integral gain K_i .

For the set of rules, a linguistic variable is assigned based on the input for each output, as shown in Table 8.

Table 8. Set of rules for selecting the gains

Reference	Gains	
R1	$K_c = M$	$K_i = S$
R2	$K_c = L$	$K_i = M$
R3	$K_c = S$	$K_i = VL$
R4	$K_c = VS$	$K_i = L$
R5	$K_c = L$	$K_i = M$

It should be recalled that it is desired to control the illuminance level in a study or working area, to maintain the 500 lx recommended by WHO. Voltage levels were used to facilitate the design of these controllers, and thus it is required to convert from voltage to illuminance. This may be carried out based on lamp

characterization, modifying the block diagram of the system as shown in Figure 16.

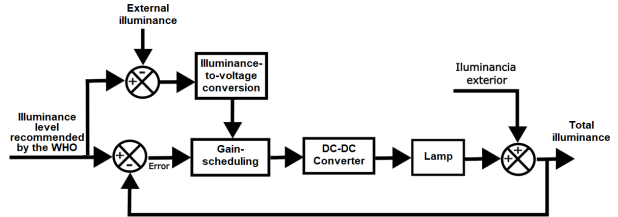


Figure 16. Block diagram of the system including the lamp

3. Results and discussion

For validating the control schemes designed, they are simulated with three different transfer functions: the intermediate transfer function, given by equation (4), and the transfer functions at the ends of the operating range of the lamp, given by equations (2) and (6).

Figure 17 shows the response obtained when simulating the intermediate transfer function with the PI controller. It is observed that there is a steady-state error of 0%, a maximum overshoot of 4.6% and a settling time of approximately 1.8 ms.

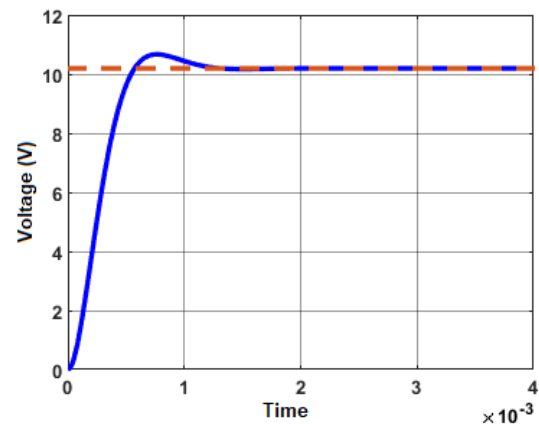


Figure 17. Response of the transfer function corresponding to the intermediate operating range with a PI control scheme

Nevertheless, some undesired dynamics appear when the same control scheme is simulated with the same gains in the operating ranges at the ends; in particular, the maximum overshoot exceeds the 12 V corresponding to the supply voltage of the lamp. The responses of these TFs under the action of the control scheme are shown in Figures 18 and 19 respectively.

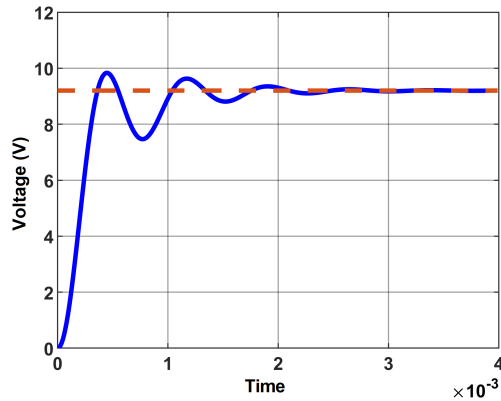


Figure 18. Response of the transfer function corresponding to the lower operating range with a PI control scheme

Although in these three cases a steady-state error of 0% is reached, an overshoot above 12 V may damage the lamp, and thus a unique PI control is not very suitable for the application.

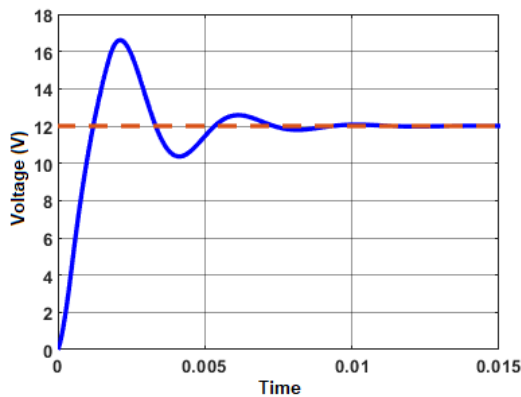


Figure 19. Response of the transfer function corresponding to the upper operating range with a PI control scheme

On the other hand, an improvement in the response within the tuning range is obtained when simulating the fuzzy PI control scheme, since the maximum overshoot is significantly reduced, as shown in Figure 20. In addition, a steady-state error of 0% is guaranteed and a settling time of 1.2 ms is achieved.

Nevertheless, undesired responses are obtained when the same controller is applied in the operating ranges at the ends, since even though there is no overshoot, the steady-state error is greater than 2%, as shown in Figures 21 and 22.

On the other hand, the desired response is obtained for each of the ranges when using the gain-scheduling control scheme. Figure 23 shows the response for the intermediate operating range, whereas the responses for the lower and upper operating ranges are shown in Figures 24 and 25, respectively.

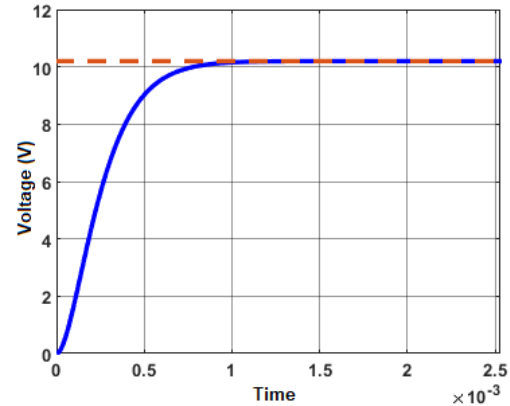


Figure 20. Response of the transfer function corresponding to the intermediate operating range with a fuzzy PI control scheme

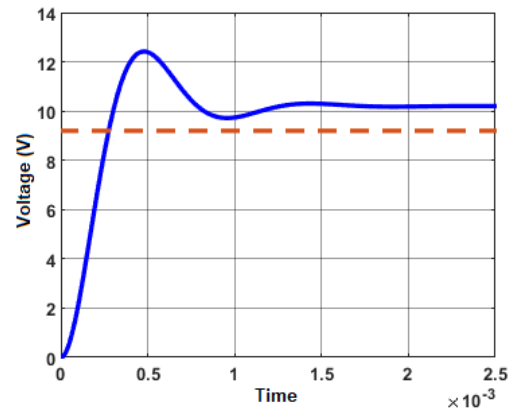


Figure 21. Response of the transfer function corresponding to the lower operating range with a fuzzy PI control scheme

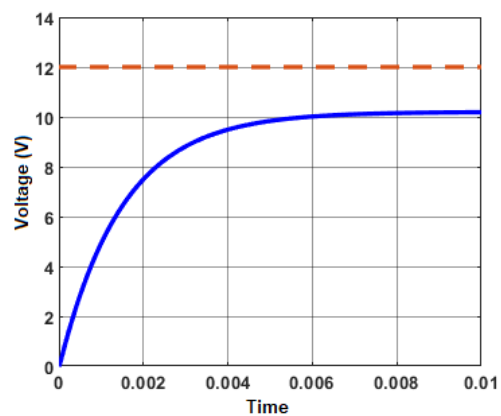


Figure 22. Response of the transfer function corresponding to the upper operating range with a fuzzy PI control scheme

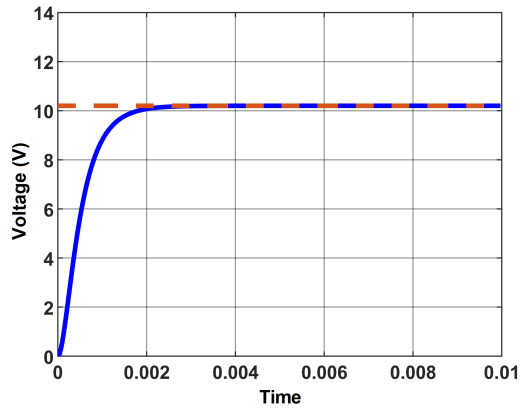


Figure 23. Response of the transfer function corresponding to the intermediate operating range with a gain-scheduling control scheme

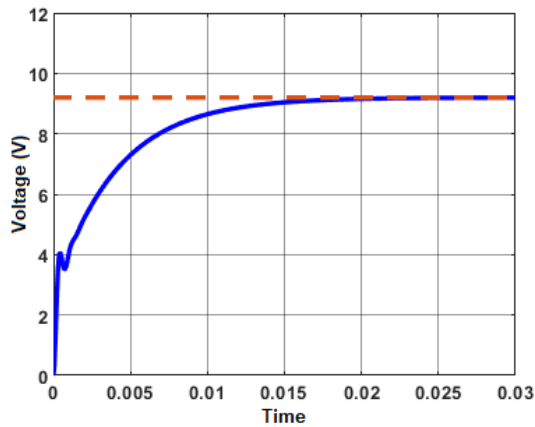


Figure 24. Response of the transfer function corresponding to the lower operating range with a gain-scheduling control scheme

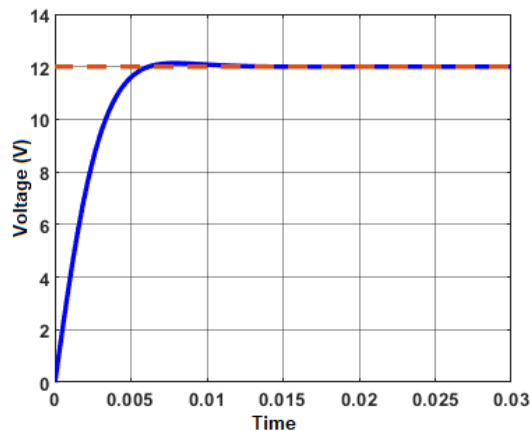


Figure 25. Response of the transfer function corresponding to the upper operating range with a gain-scheduling control scheme

It is seen that all responses have a steady-state error of 0%, and maximum overshoots smaller than 2%. However, the settling time increases.

A comparison of the responses obtained with the three control schemes is shown in Table 9.

Table 9. Comparison of the responses obtained with the PI, fuzzy PI and gain-scheduling control schemes

Parameter	Control scheme	Range: 9.2 V - 9.7 V	Range: 10.2 V - 10.7 V	Range: 11.3 V - 12 V
Setting time	PI Control	3.95 ms	1.8 ms	13 ms
	Fuzzy PI Control	2.2 ms	1.2 ms	9 ms
	Gain scheduling	24 ms	3 ms	12 ms
Maximum overshoot	PI Control	6.78 %	4.6 %	38.42 %
	Fuzzy PI Control	35%	0%	0%
	Gain scheduling	0%	0%	1.08 %
Steady-state error	PI Control	0%	0%	0%
	Fuzzy PI Control	10.86 %	0%	15%
	Gain scheduling	0%	0%	0%

It is important to mention that the maximum overshoot and the settling time for which the gain-scheduling control was tuned are different from the design specifications. This is mainly due to the effects of the real pole and the zero that appears when the loop is closed.

However, these effects do not harm the desired dynamics but benefit it, achieving very small overshoots. The effect of the real pole and the zero is mostly noted in the settling time; however, this time is in the order of milliseconds, which for the case of lighting and of the converter is not relevant.

Based on the above, the gain-scheduling control shows a better response in the entire operating range of the lamp, and thus the simulations incorporate the model of the lamp. The external illuminance pattern is taken from the levels of solar irradiance during a spring day, in the city of Cuernavaca, Morelos, Mexico, collected from the database of the Instituto Nacional de Ecología y Cambio Climático [21]. This pattern is shown in Figure 26.

The eye protection lamp should supplement the lighting in the case of changes in the external illuminance, in order to maintain the 500 lx recommended by the WHO. The response of the system in the presence of variations in the external illuminance is shown in Figure 27.

It is seen that despite the changes in the external lighting, the level of total illuminance is maintained at the 500 lx recommended by the WHO. However, it is observed a higher ripple when the external lighting is minimum. This ripple is shown in Figure 28, and it appears because at this point the converter should supply a higher voltage to the lamp, and consequently there is a higher voltage ripple due to the effects of the converter output capacitor. However, this ripple

is around 1 %, which is within the margins that are acceptable from the point of view of control theory.

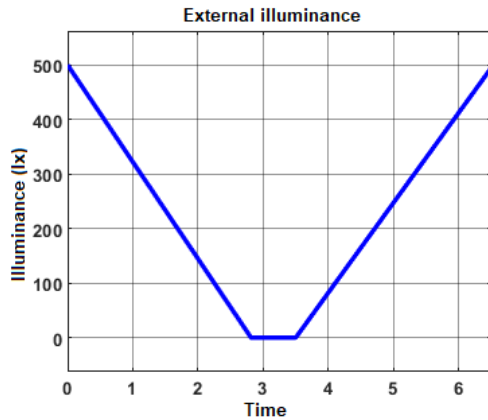


Figure 26. Pattern of external illuminance

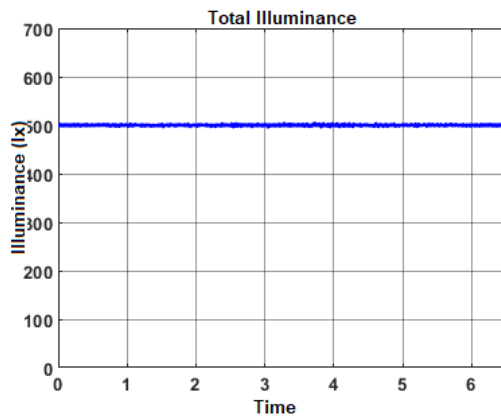


Figure 27. Total illuminance of the system

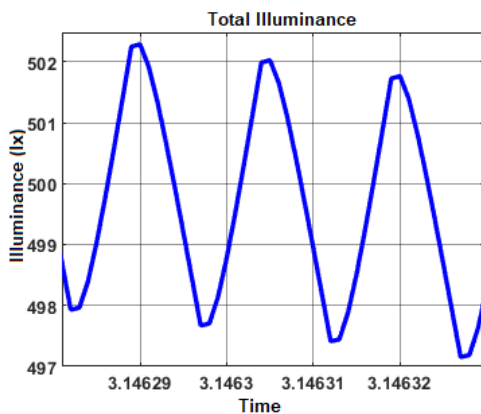


Figure 28. Effects of the voltage ripple on the illuminance

On the other hand, Figure 29 shows the voltage supplied by the designed converter. It is seen that the voltage remains within the operating ranges, which guarantees not damaging the lamp. In addition, it is

shown that the lamp does not work in a single operating point, but it demands different voltage levels to the converter according to the changes in the level of external illuminance.

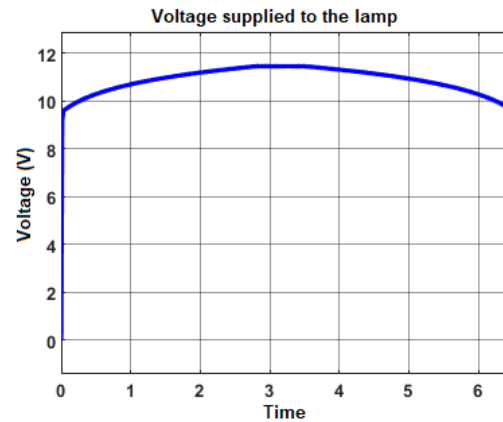


Figure 29. Voltage supplied to the lamp by the DC-DC converter

4. Conclusions

At present, there are different applications of LED lamps. Some of them require precision when varying the light intensity, such as eye protection lamps.

For that reason, this work presented the simulation of a DC-DC converter with three control schemes, which vary the illuminance of an eye protection lamp to maintain the 500 lx recommended by the WHO to prevent eye diseases, and considering that external light sources disturb the lighting provided by the lamp.

A classical PI control scheme is capable of guaranteeing a steady-state error of 0 % in the entire operating range of the lamp, but it does not guarantee appropriate levels of maximum overshoot.

On the other hand, the designed fuzzy PI control scheme is capable of guaranteeing that the voltage levels supported by the lamp are not exceeded; however, if the operating point changes the steady-state error increases.

Conversely, the designed gain-scheduling control scheme is a combination of the PI and fuzzy logic controllers, where the latter is used as gain selector to enable the adjustment of the controller gain depending on the operating point of the system. In this manner, it is guaranteed to have a steady-state error of 0 % and to reduce as much as possible the maximum overshoot.

In the simulation of the gain-scheduling control scheme including the model of the lamp, it was possible to maintain the illuminance level at 500 lx, and thus the lamp supplements external lighting to fulfill the recommendation by the WHO. In addition, it is guaranteed that the DC-DC converter does not supply voltage levels that exceed the operating range of the

lamp, and thus it is verified that the light intensity of the LED lamp is regulated precisely and guaranteed not to damage it, as opposed to other works that focus on the control at only one operating point using a linear controller.

As a future work, it is worth mentioning that it is possible to improve the ripple present in the total illuminance, by increasing the capacitance value of the converter output capacitor; however, this modifies the TFs, and thus the dynamics obtained.

On the other hand, gain-scheduling control may be incorporated in different applications, and it is thus recommended its validation with other case studies related to lighting applications.

References

- [1] M. C. Gutiérrez Hernández, “Iluminación LED. ahorro, eficiencia e innovación. Proyecto de mejora de la iluminación de un hotel,” Universidad de la Laguna, España, 2015. [Online]. Available: <https://bit.ly/3uM3vie>
- [2] N. Pai and S. G. Kini, “Design and prototyping of dimmable LED driver for general lighting application,” in *2018 Second International Conference on Electronics, Communication and Aerospace Technology (ICECA)*, 2018, pp. 1–6. [Online]. Available: <https://doi.org/10.1109/ICECA.2018.8474548>
- [3] F. Bento and A. J. M. Cardoso, “Comprehensive survey and critical evaluation of the performance of state-of-the-art LED drivers for lighting systems,” *Chinese Journal of Electrical Engineering*, vol. 7, no. 2, pp. 21–36, 2021. [Online]. Available: <https://doi.org/10.23919/CJEE.2021.000013>
- [4] S. Iturriaga-Medina, P. Martínez-Rodríguez, M. Juárez-Balderas, J. Sosa, and C. Limones, “A buck converter controller design in an electronic drive for LED lighting applications,” in *2015 IEEE International Autumn Meeting on Power, Electronics and Computing (ROPEC)*, 2015, pp. 1–5. [Online]. Available: <https://doi.org/10.1109/ROPEC.2015.7395105>
- [5] M. Juárez, P. Martínez, G. Vázquez, J. Sosa, X. Prieto, and R. Martínez, “Analysis of buck converter control for automobile LED headlights application,” in *2014 IEEE International Autumn Meeting on Power, Electronics and Computing (ROPEC)*, 2014, pp. 1–4. [Online]. Available: <https://doi.org/10.1109/ROPEC.2014.7036298>
- [6] M. D. Vijay, K. Shah, G. Bhuvaneshwari, and B. Singh, “LED based street lighting with automatic intensity control using solar PV,” in *2015 IEEE IAS Joint Industrial and Commercial Power Systems / Petroleum and Chemical Industry Conference (ICPSP-CIC)*, 2015, pp. 197–202. [Online]. Available: <https://doi.org/10.1109/CICPS.2015.7974074>
- [7] X. He, H. Wang, J. Cao, and D. Lei, “Design of high-power LED automatic dimming system for light source of on-line detection system,” in *2020 IEEE 5th Information Technology and Mechatronics Engineering Conference (ITOEC)*, 2020, pp. 1487–1491. [Online]. Available: <https://doi.org/10.1109/ITOEC49072.2020.9141898>
- [8] N. K. Kandasamy, G. Karunagaran, C. Spanos, K. J. Tseng, and B.-H. Soong, “Smart lighting system using ANN-IMC for personalized lighting control and daylight harvesting,” *Building and Environment*, vol. 139, pp. 170–180, 2018. [Online]. Available: <https://doi.org/10.1016/j.buildenv.2018.05.005>
- [9] R. B. Caldo, J. T. Seranilla, D. J. Castillo, K. S. Diocales, W. D. Gulle, B. L. Núñez, and C. T. Parreño, “Design and development of fuzzy logic controlled dimming lighting system using arduino microcontroller,” in *2015 International Conference on Humanoid, Nanotechnology, Information Technology, Communication and Control, Environment and Management (HNICEM)*, 2015, pp. 1–6. [Online]. Available: <https://doi.org/10.1109/HNICEM.2015.7393161>
- [10] M. G. Shafer, E. Saputra, K. A. Bakar, and F. Ramadhani, “Modeling of fuzzy logic control system for controlling homogeneity of light intensity from light emitting diode,” in *2012 Third International Conference on Intelligent Systems Modelling and Simulation*, 2012, pp. 71–75. [Online]. Available: <https://doi.org/10.1109/ISMS.2012.90>
- [11] D. T. Phan, N. T. Bui, T. H. Vo, S. Park, J. Choi, S. Mondal, B.-G. Kim, and J. Oh, “Development of a LED light therapy device with power density control using a fuzzy logic controller,” *Medical Engineering & Physics*, vol. 86, pp. 71–77, 2020. [Online]. Available: <https://doi.org/10.1016/j.medengphy.2020.09.008>
- [12] X. He, C. Huang, Y. Li, H. Wang, D. Lei, and M. Yao, “An adaptive dimming system of high-power led based on fuzzy pid control algorithm for machine vision lighting,” in *2020 IEEE 4th Information Technology, Networking, Electronic and Automation Control Conference (ITNEC)*, vol. 1, 2020, pp. 2198–2202. [Online]. Available: <https://doi.org/10.1109/ITNEC48623.2020.9084741>
- [13] R. Gil Bernal and D. F. Díaz Caro, “Driver de potencia dimerizable para un arreglo de LED,” 2017. [Online]. Available: <https://bit.ly/3WhnzVs>

- [14] M. Lara Ortiz, J. Garrido Jurado, M. L. Ruz Ruiz, and F. Vázquez Serrano, “Control PI adaptativo por ganancia programada del nivel de un tanque de sección trapezoidal,” in *XXXIX Jornadas de Automática*. XXXIX Jornadas de Automática, 2018, pp. 444–451. [Online]. Available: <https://doi.org/10.17979/spudc.9788497497565>
- [15] J. A. Brizuela-Mendoza, A. Zavala-Río, and C. M. Astorga-Zaragoza, “Controlador de ganancias programadas aplicado a la estabilización de una bicicleta sin conductor,” in *Congreso Nacional de Control Automático*, 2013, pp. 36–41. [Online]. Available: <https://bit.ly/3BxfofX>
- [16] OMS. (2019) La OMS presenta el primer informe mundial sobre la visión. [Online]. Available: <https://bit.ly/3YwQneO>
- [17] B. A. Holden, T. R. Fricke, D. A. Wilson, M. Jong, K. S. Naidoo, P. Sankaridurg, T. Y. Wong, T. J. Naduvilath, and S. Resnikoff, “Global prevalence of myopia and high myopia and temporal trends from 2000 through 2050,” *Ophthalmology*, vol. 123, no. 5, pp. 1036–1042, Feb. 2016. [Online]. Available: <https://doi.org/10.1016/j.ophtha.2016.01.006>
- [18] Y. Xiaogang, W. Wang, and L. Fenna, “Design and simulation of intelligent dimmer based on fuzzy PID,” in *2020 International Conference on Intelligent Design (ICID)*, 2020, pp. 86–89. [Online]. Available: <https://doi.org/10.1109/ICID52250.2020.00025>
- [19] R. A. Gamboa López, “Asistente para el diseño y simulación de convertidores CD-CD en lazo cerrado,” Master’s thesis, 2018. [Online]. Available: <https://bit.ly/3iVLSKl>
- [20] S. González de León, “Control PID con sintonización difusa y control difuso,” Master’s thesis, 2013. [Online]. Available: <https://bit.ly/3Fpn3hC>
- [21] INECC. (2019) Datos Estación Cuernavaca. Instituto Nacional de Ecología y Cambio Climático. [Online]. Available: <https://bit.ly/2wGUPvC>